Retrieval of Snow Grain Size and Impurity from GLI: Atmospheric Correction

Knut Stamnes and Wei Li

Light and Life Laboratory
Department of Physics & Engineering Physics
Stevens Institute of Technology
Hoboken, NJ 07030

ADEOS-II/GLI Workshop · Tokyo · November 2001

OUTLINE OF TALK

- Brief Overview of Theoretical Aspects and Retrieval Principles:
  => Which GLI Channels Do We Use and Why?
  => Short Description of Retrieval Procedure.
- Atmospheric Correction and Retrieval Products:
  => Cloud Mask
  => Aerosol Model and Optical Depth
  => Snow Grain Size and Impurities
  => Spectral Snow Albedo
- Algorithm Testing and Validation:
  => Use of Synthetic Data – Numerical Testbed
  => Testing Against MODIS Data
  => Field Validations Ultimately Required
- Summary

Light and Life Laboratory STEVENS Institute of Technology

Theoretical Aspects and Retrieval Principles (1)

Our algorithm development is based on:

- **the discrete-ordinate-method (DISORT) [see Refs. 2-4] to compute the top-of-the-atmosphere (TOA) radiances, because:**

=> this method allows radiances to be computed at arbitrary user-specified polar and azimuthal angles.

We expand the phase function as:

$$p(\tau, \cos\Theta) = p(\tau, u', \phi'; u, \phi) = \sum_{m=0}^{2M-1} (2 - \delta_{0,m}) p^m(u', u) \cos m(\phi' - \phi) \qquad (1)$$

$p^m(u', u) = \Sigma_{l=m}^{2M-1} (2l+1) g_l(\tau) \Lambda_l^m(u') \Lambda_l^m(u)$; $\Lambda_l^m(u) = \sqrt{(l-m)!/(l+m)!} P_l^m(u)$;

$g_l(\tau) = \frac{1}{2} \int_{-1}^{+1} P_l(\cos\Theta) p(\tau, \cos\Theta) d(\cos\Theta)$; τ **is the vertical optical depth;** $(u' = \cos\theta', \phi')$ **and** $(u = \cos\theta, \phi)$ **are the cosine of the polar angle and the azimuthal angle, before and after the scattering, respectively.**

Theoretical Aspects and Retrieval Principles (2)

- **Since Eq. (1) is a Fourier cosine series, we expand the radiance in the same way:**

$$I(\tau, u, \mu_0, \Delta\phi) = \sum_{m=0}^{2M-1} I^m(\tau, u, \mu_0) cos(m\Delta\phi) \qquad (2)$$

  - $\mu_0 = cos\theta_0$ **is the cosine of the solar zenith angle** θ_0
  - $\Delta\phi = \phi_0 - \phi$ **is the relative azimuth angle between the incident solar beam direction** ϕ_0 **and the sensor viewing direction** ϕ
  - $I(\tau, \mu_0, u, \Delta\phi)$ **is the radiance**
  - $I^m(\tau, \mu_0, u)$ **is the** m-th **Fourier component of the radiance**

- **Each Fourier component satisfies the radiative transfer equation:**

$$u\frac{I^m(\tau, u, \mu_0)}{d\tau} = I^m(\tau, u, \mu_0) - \frac{a(\tau)}{2}\int_{-1}^{1} p^m(u, u')I^m(\tau, u')du' - Q^m(\tau, u) \qquad (3)$$

- **Solution of Eq. (3) for each** m **yields** $I^m(\tau, u, \mu_0)$**, and substitution in Eq. (2) yields** $I(\tau, u, \mu_0, \Delta\phi)$**.**

Light and Life Laboratory STEVENS Institute of Technology

Theoretical Aspects and Retrieval Principles (3)

- **We store the $I^m(\tau, u, \mu_0)$ terms [see Eq. (2)] in the lookup table.**
- **The TOA radiance $I(\tau, u, \mu_0, \Delta\phi)$ is then computed based on Eq. (2) using an interpolation method.**
- **We employ a** *cubic spline interpolation* **method [see Ref. 5] for the polar and solar zenith angle dependence of the radiance.**
- **Use of Eq. (2) implies an accurate analytic treatment of the azimuth dependence of the radiance.**

Light and Life Laboratory STEVENS Institute of Technology

Reflected radiances in Channels 5 and 26

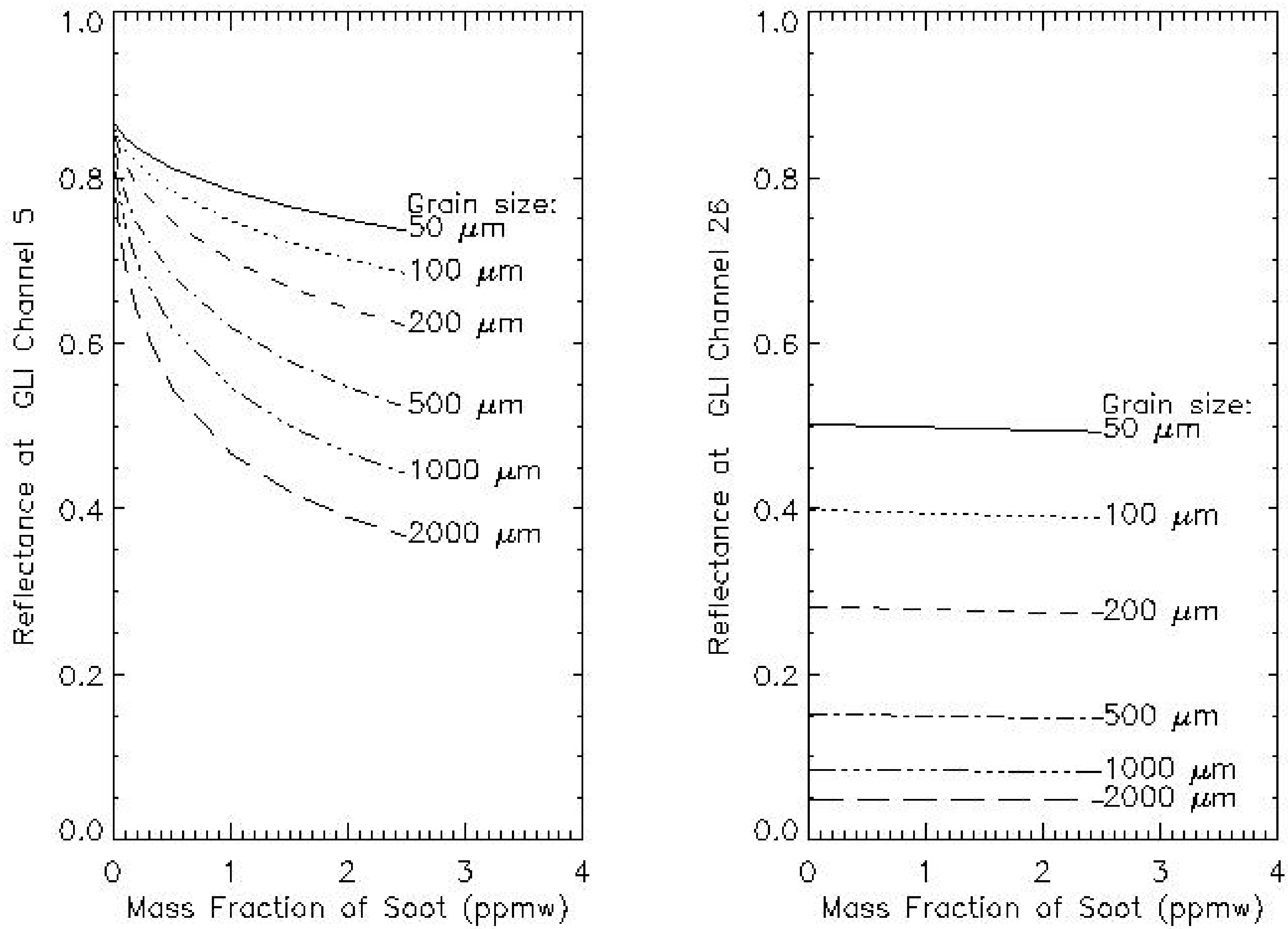

Figure 1: Reflected radiances in channels 5 and 26 as a function of mass fraction of soot and grain size.

Flow Chart of Retrieval Algorithm

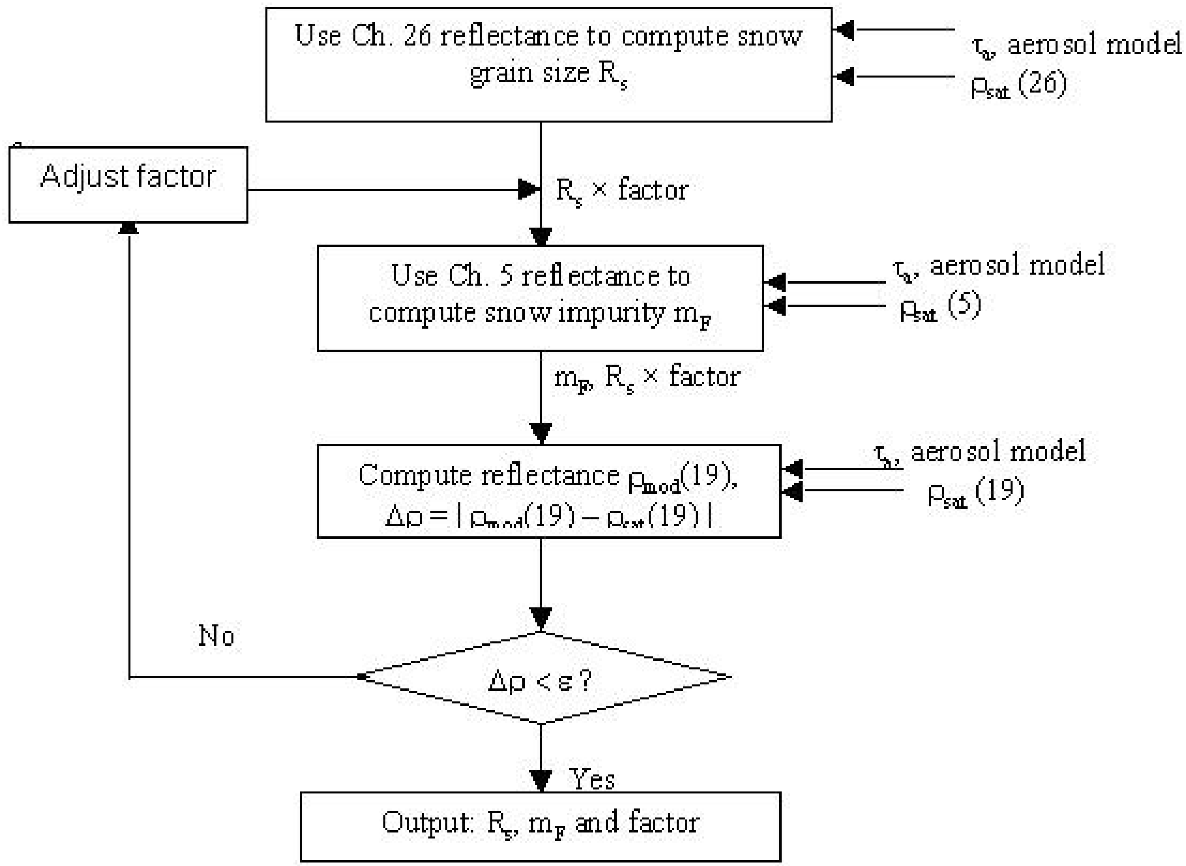

Figure 2.2 Flow chart of the retrieval algorithm for snow grain size and impurity concentration. τ_a is the aerosol optical depth, Rs the snow grain size, and m_F the impurity concentration. The $\rho_{sat}(26)$, $\rho_{sat}(19)$, and $\rho_{sat}(5)$ are the satellite-measured reflectances at GLI channels 26, 19 and 5, respectively. The $\rho_{mod}(19)$ is the computed reflectance (from lookup table) at GLI channel 19.

Wavelength-dependence of Photon Penetration Depth (see Ref. 1)

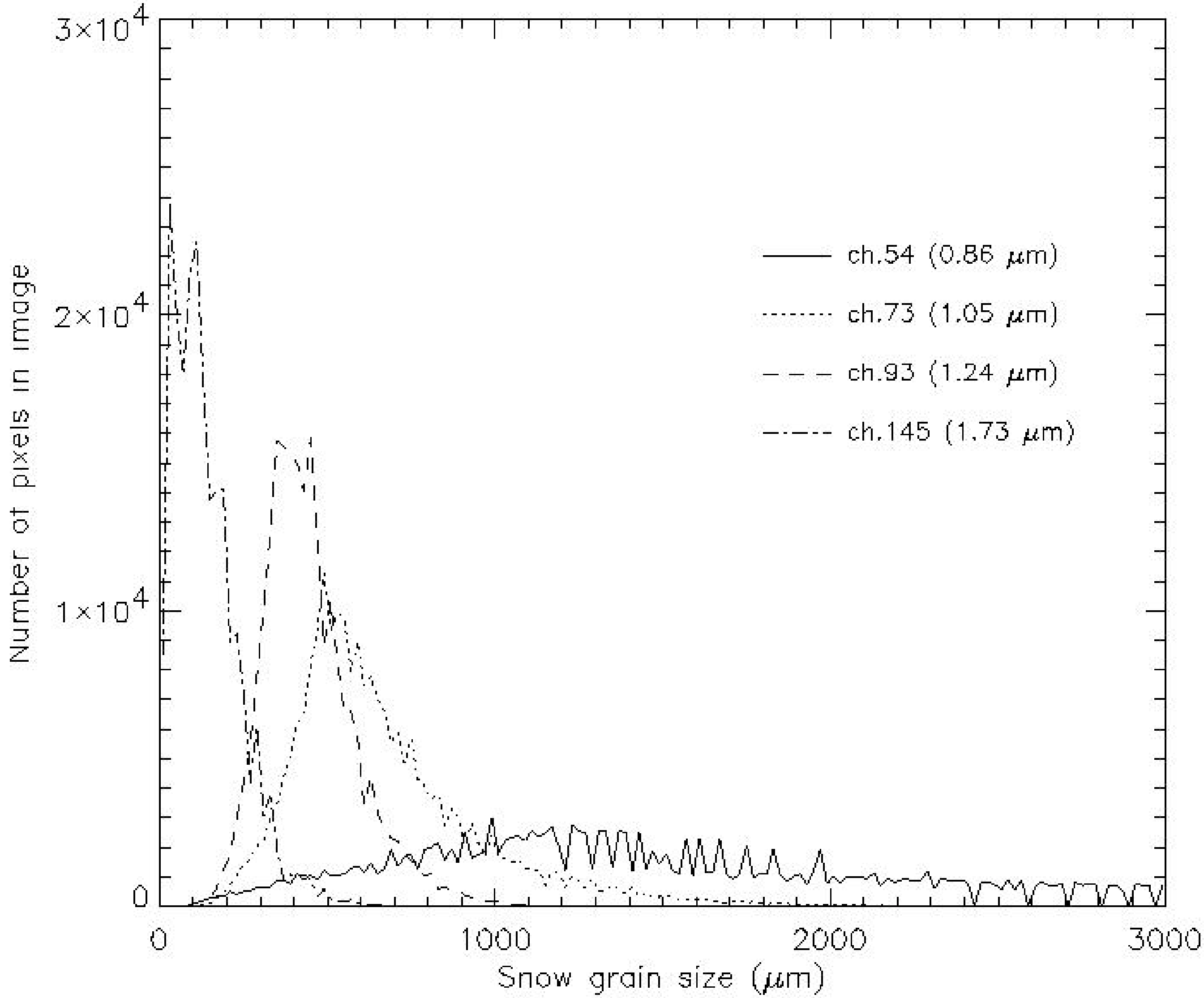

Figure 2: Histograms of retrieved snow grain size from AVIRIS channels 54, 73, 93, and 145.

Atmospheric Correction (1)

Atmospheric Correction means Removal of Aerosol Contribution to TOA Radiance, because:

- **Rayleigh scattering can be computed accurately;**
- **absorption by trace gases is unimportant in channels 1 and 5.**

Removal of the aerosol contribution to TOA radiance is difficult:

- **large spatial and temporal variation in aerosol properties**
- **high albedo of snow surface.**
- **Use of incorrect aerosol model implies TOA reflectance errors:**
  - **as large as 20% for weakly-absorbing aerosols;**
  - **an error of 50% or more for strongly absorbing aerosols.**
- **Such large errors will cause a failure of the retrieval of snow grain size and impurity.**
- **Proper selection of aerosol model is critically important for accurate retrieval of snow grain size and impurity.**

Atmospheric Correction (2)

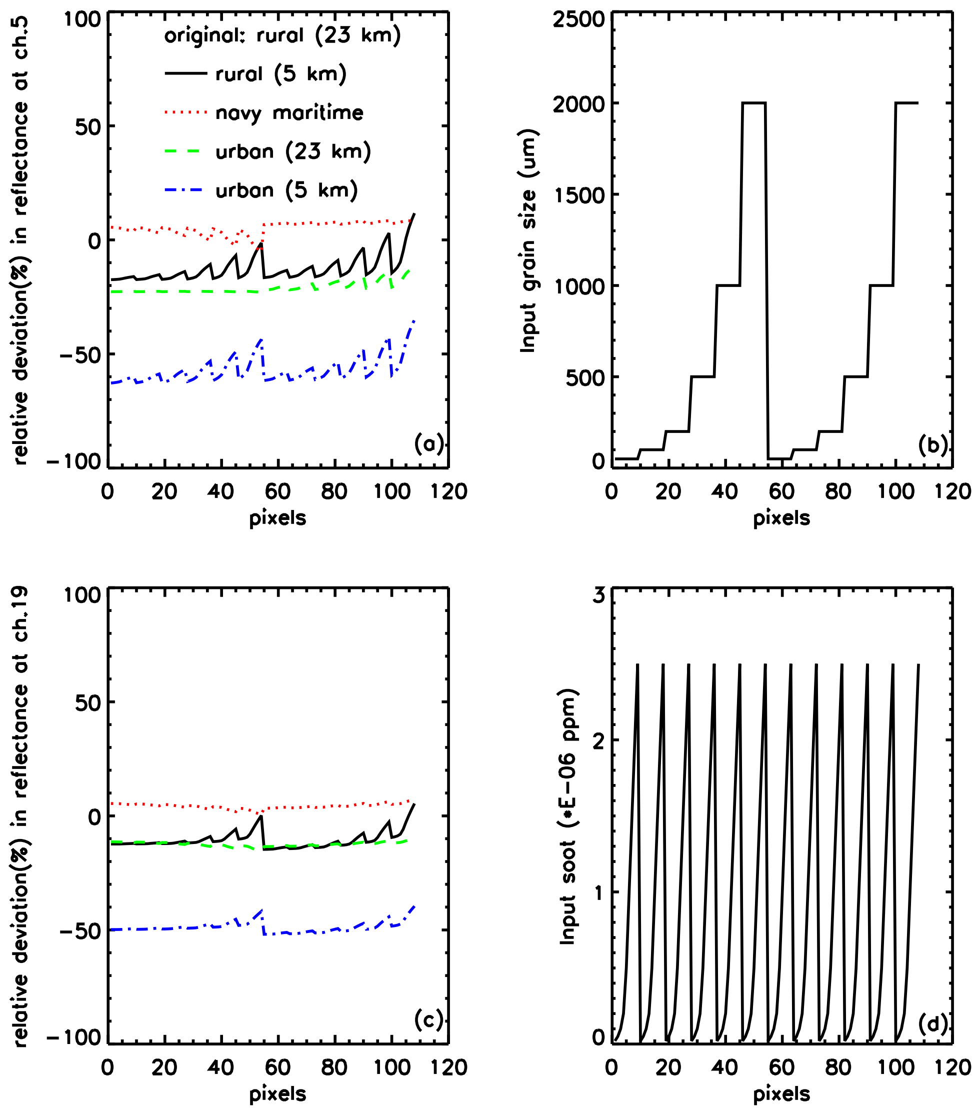

Figure 3: Relative deviations in TOA reflectance in GLI channels 5 and 19 resulting from use of wrong aerosol models. The right panels contain the input grain size and impurity for each test pixel.

Atmospheric Correction (3)

How Can We Do Atmospheric Correction over Bright Surfaces like Snow? The Answer is:

- **the reflectance in channel 5** *decreases* **almost linearly with optical depth when the albedo is** *higher* **than about 0.5;**

Note also that:

- **the reflectance in channel 5** *increases* **almost linearly with optical depth when the albedo is** *lower* **than about 0.5.**

Hence:

- **Aerosol Removal is Feasible over Bright as Well as Dark Surfaces!!**

Light and Life Laboratory STEVENS Institute of Technology

Atmospheric Correction (4)

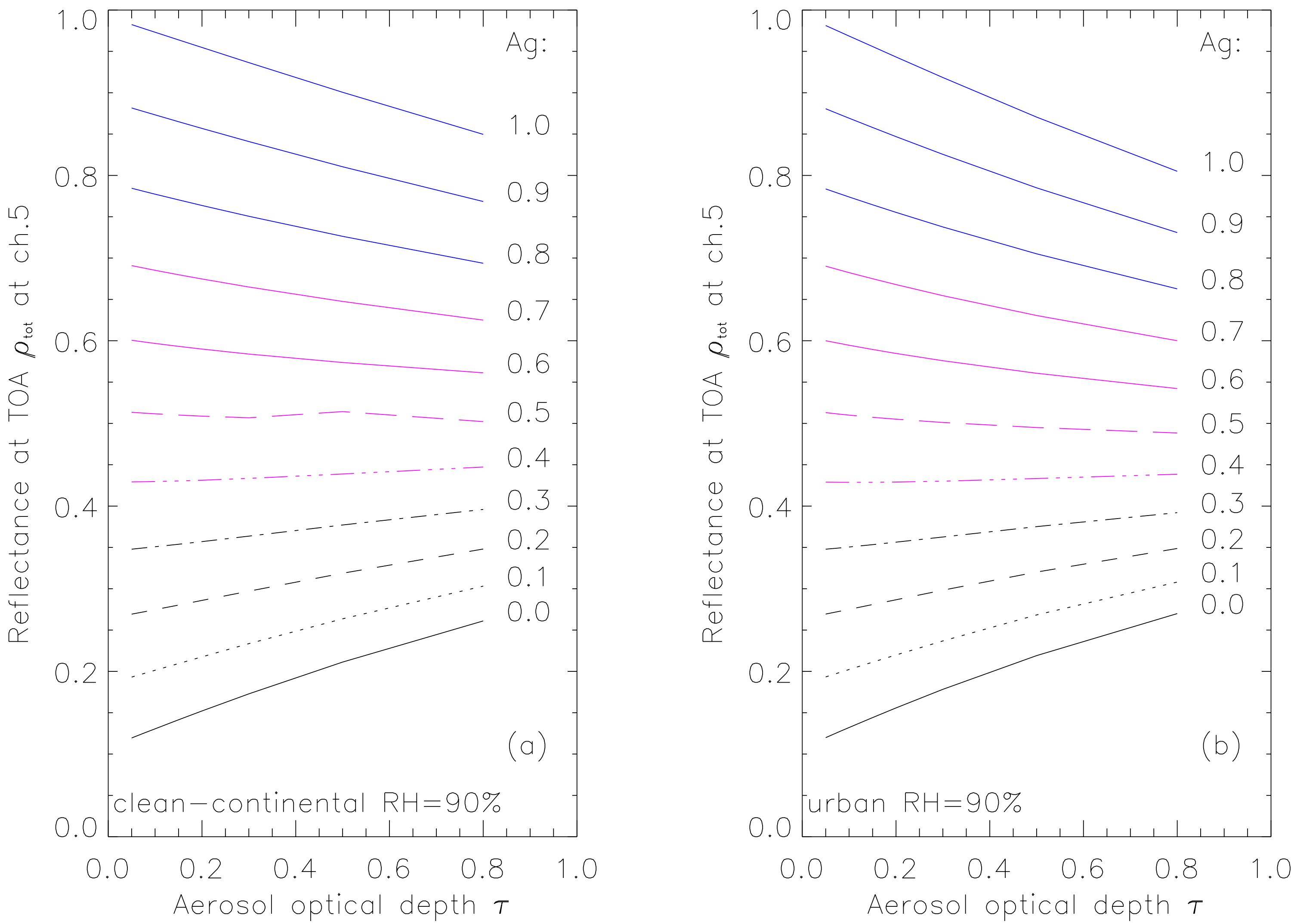

Figure 4: TOA reflectance at GLI channel 5 as a function of aerosol optical depth and surface reflectance. (a): non-absorbiing aerosols; (b): absorbing aerosols.

Atmospheric Correction (5)

For a Lambertian surface the reflectance is given exactly by:

$$\rho_{tot}(\theta_v, \rho_{sur}) = \rho_{atm}(\theta_v, \rho_{sur} = 0) + \frac{\rho_{sur} \cdot \mathcal{T}(\theta_s) \cdot \tilde{\mathcal{T}}(\theta_v)}{\pi(1 - \rho_{sur} \cdot \bar{\tilde{\rho}}\ )}. \tag{4}$$

where

- θ_s = solar zenith angle; θ_v = polar viewing angle;
- $\mathcal{T}(\theta_s)$ = diffuse transmittance for illumination of the atmosphere from *above*;
- $\tilde{\mathcal{T}}(\theta_v)$ = diffuse transmittance for illumination of the atmosphere from *below*;
- $\bar{\tilde{\rho}}$ = spherical albedo for illumination of the atmosphere from *below*;

Solving for ρ_{sur}, we find:

$$\rho_{sur} = \rho_c/(1 + \rho_c \cdot \bar{\tilde{\rho}}\ ) \tag{5}$$

where

$\rho_c = \pi[\rho_{tot} - \rho_{atm}]/\mathcal{T}(\theta_s) \cdot \tilde{\mathcal{T}}(\theta_v)$.

Atmospheric Correction (6)

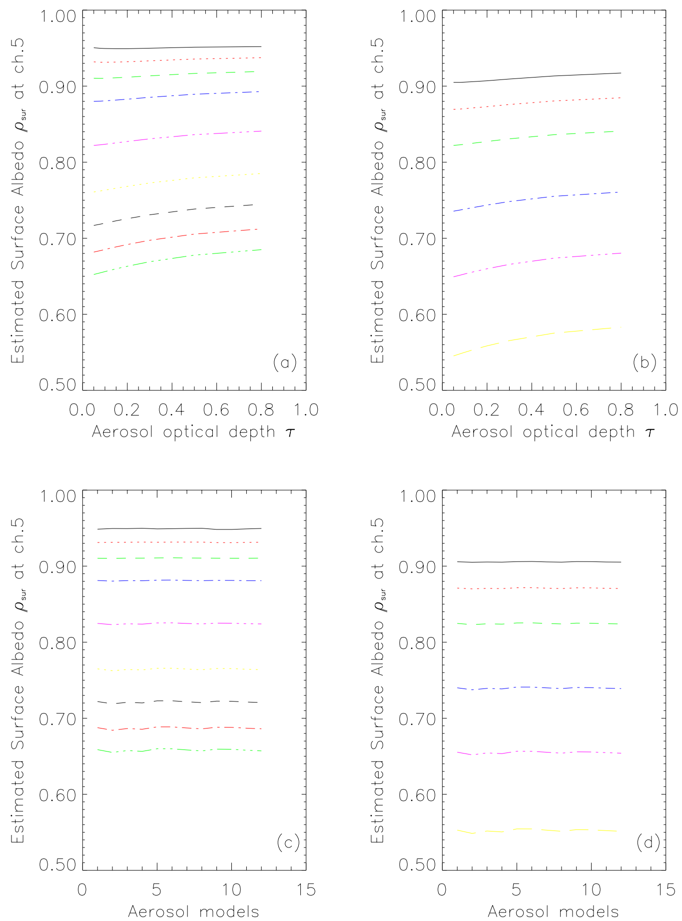

Figure 5: Retrieved Lambertian albedo ρ_{sur} as a function of aerosol optical depth [(a) and (b)], and as a function of aerosol model [(c) and (d)].

Atmospheric Correction (7)

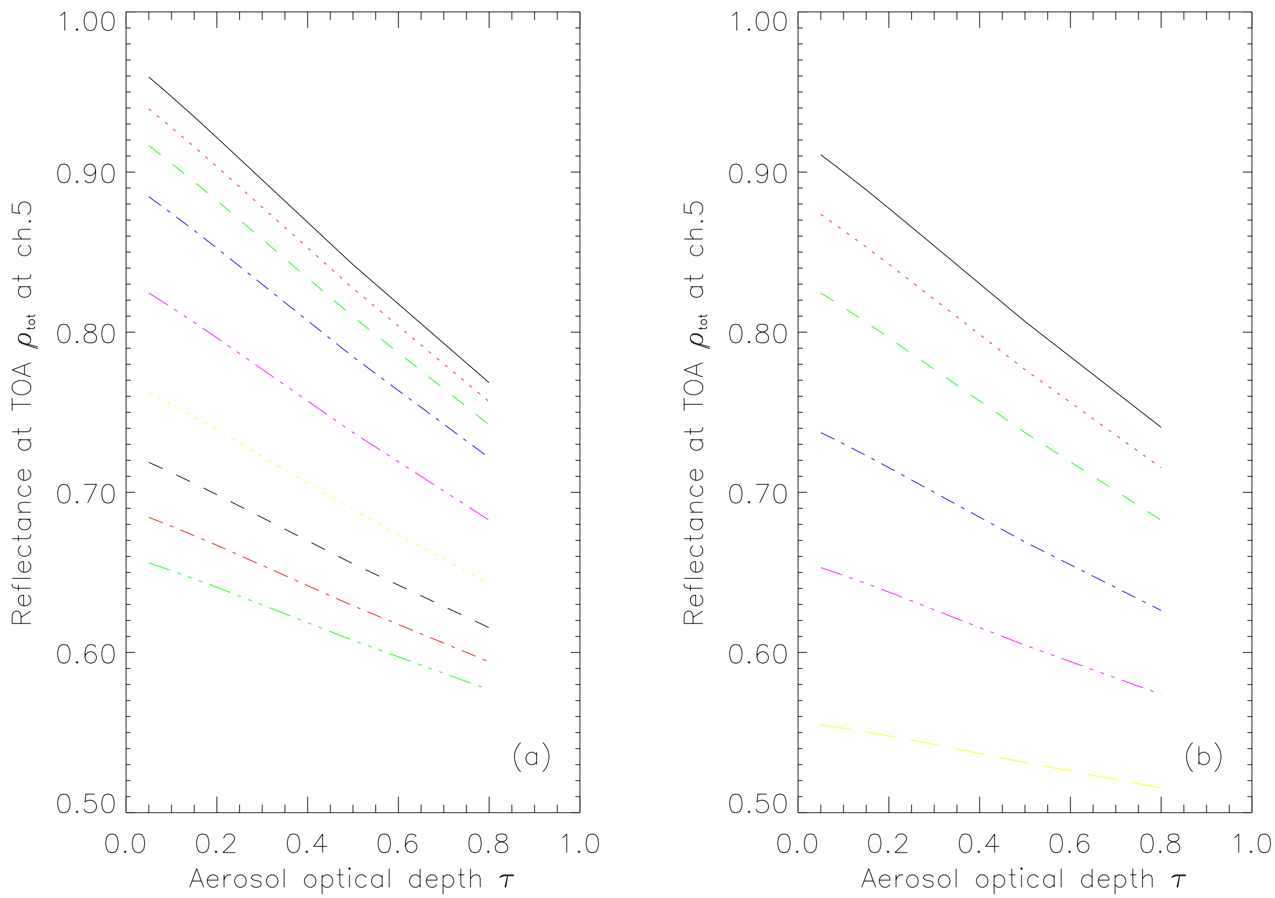

Figure 6: TOA reflectance ρ_{tot} as a function of aerosol optical depth for model "average-continental" (RH = 70%). (a): snow grain size = 200 μm and snow impurities (from top to bottom): 0.02, 0.05, 0.1, 0.2, 0.5, 1.0, 1.5 2.0, 2.5 $\times 10^{-6}$ ppmw (parts per million by weight). (b): snow impurity = 0.2 $\times 10^{-6}$ ppmw and snow grain size (from top to bottom): 50, 100, 200, 500, 1000, 2000 μm.

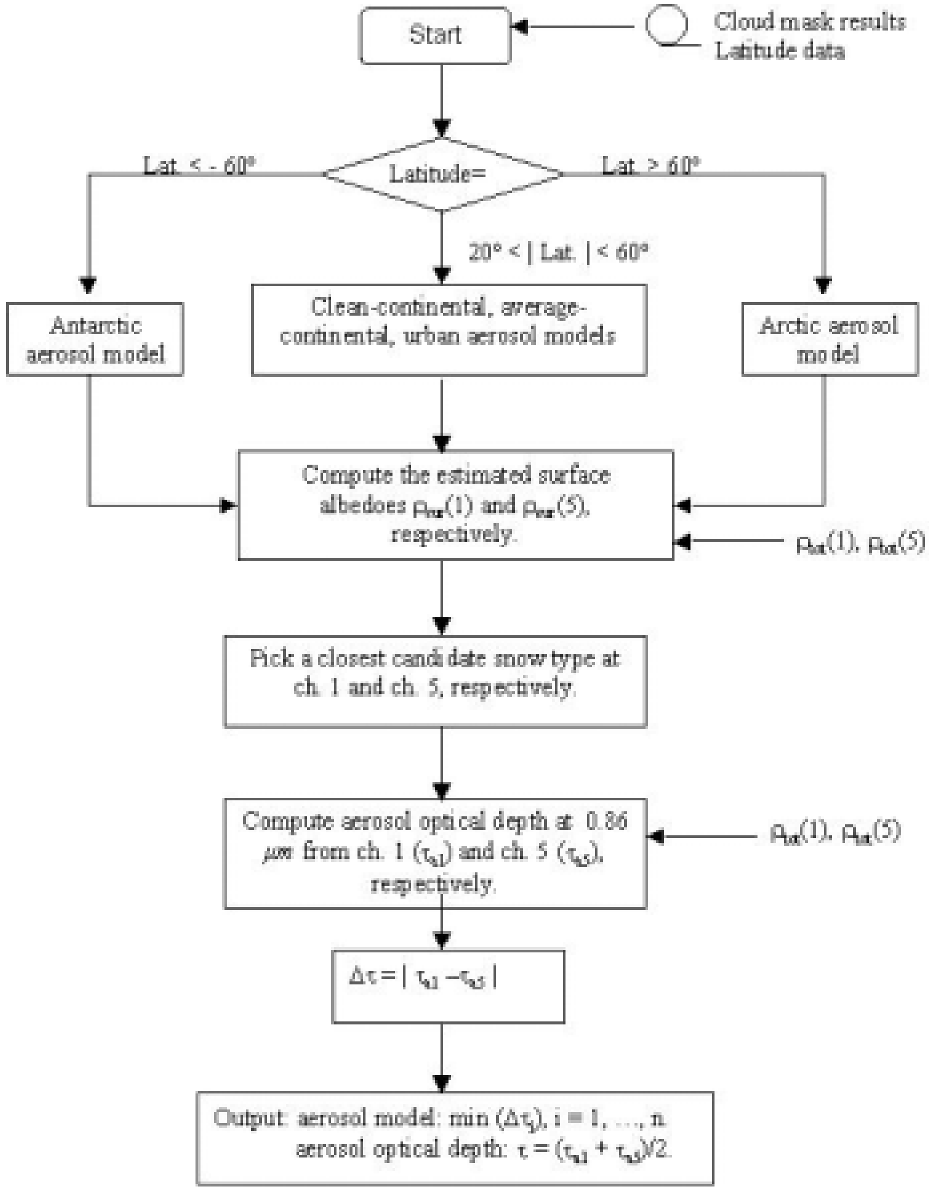

Figure 2.9 Flow chart of aerosol model and aerosol optical depth retrieval. $\rho_{tot}(1)$ and $\rho_{tot}(5)$ are the TOA reflectances of GLI channels 1 (0.38 μm) and 5 (0.46 μm), respectively. $\rho_{sur}(1)$ and $\rho_{sur}(5)$ are the Lambertian surface albedo values at GLI channels 1 and 5, respectively. The τ_{a1} and τ_{a5} are the aerosol optical depth τ (0.86) retrieved from GLI channels 1 and 5, respectively, and n is the total number of candidate aerosol models.

Validation – Synthetic Data (1)

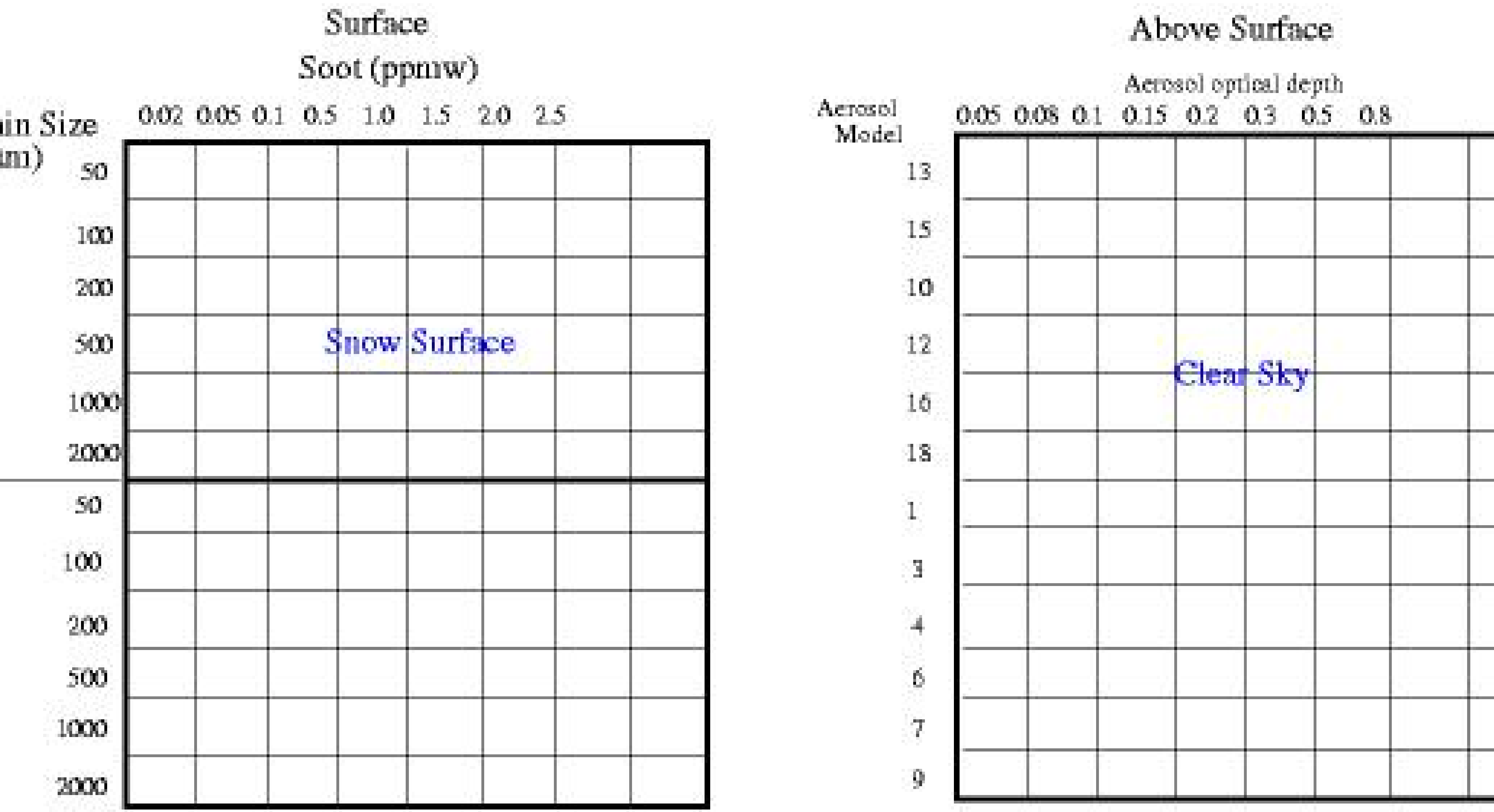

Figure 7: The structure of the GLI image.

Validation – Synthetic Data (2)

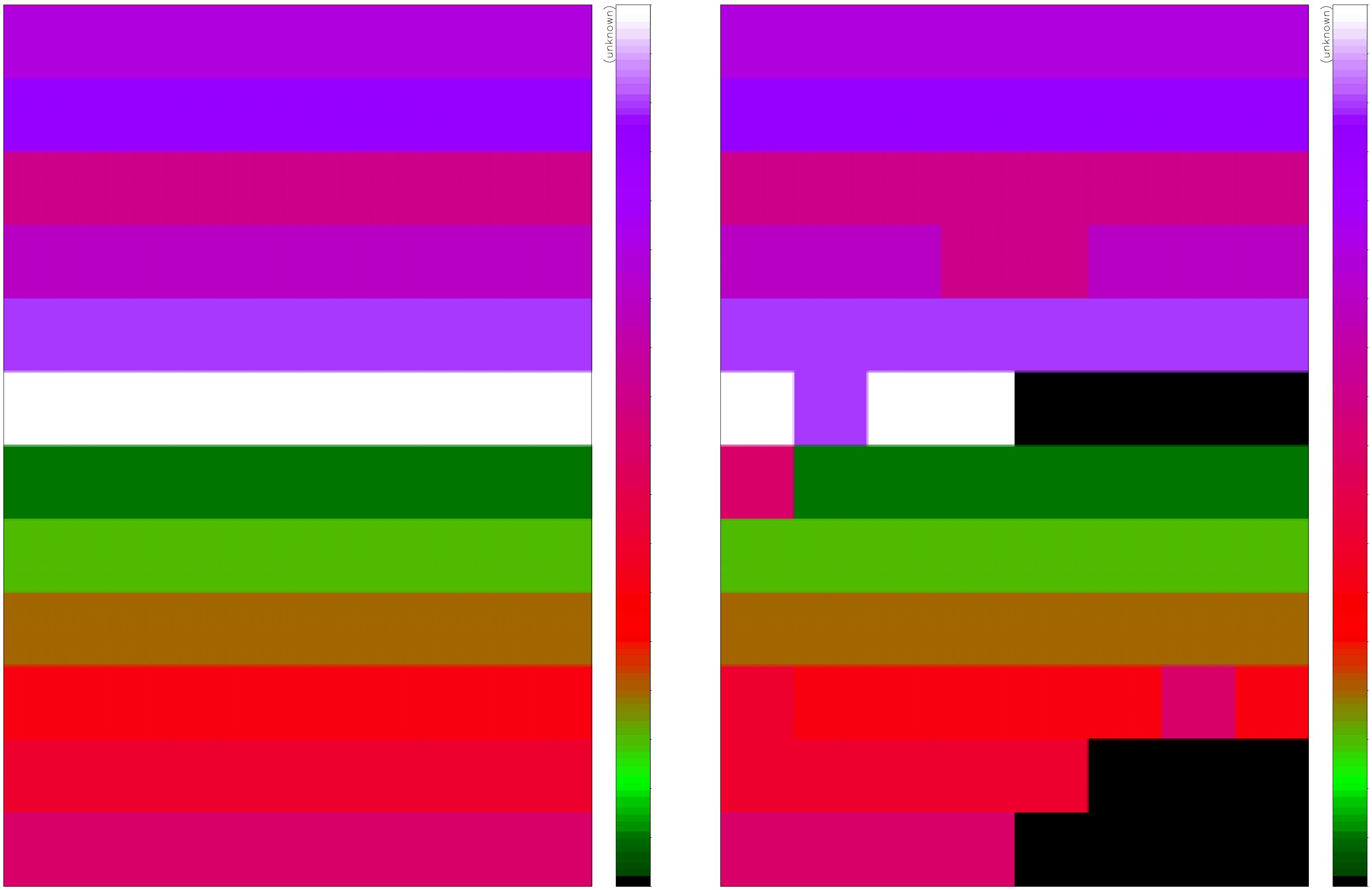

Figure 8: Aerosol Model. LEFT PANEL: Input data. RIGHT PANEL: Retrieved results.

Validation – Synthetic Data (3)

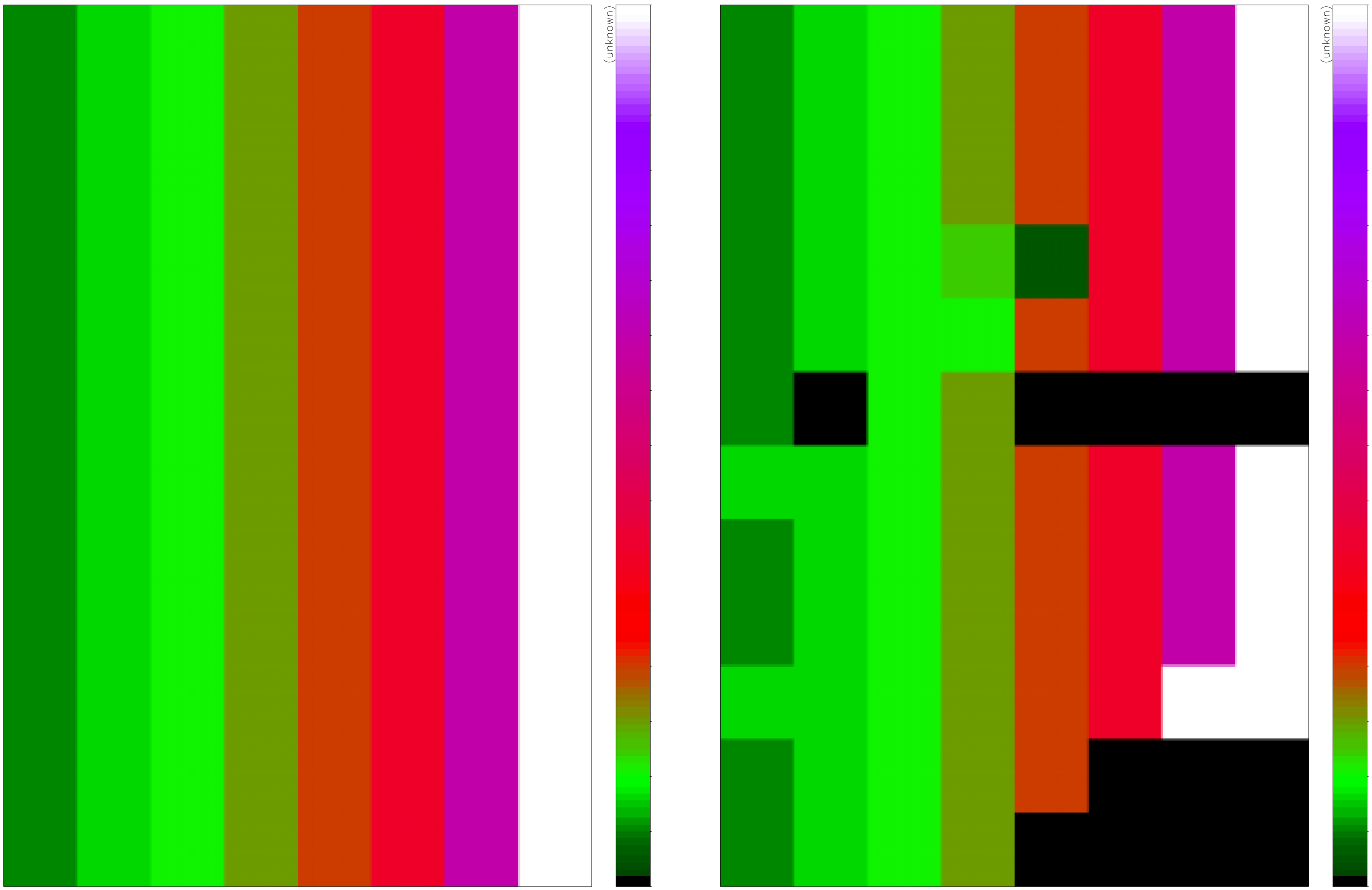

Figure 9: Aerosol Optical Depths. LEFT PANEL: Input data. RIGHT PANEL: Retrieved results.

Validation – Synthetic Data (4)

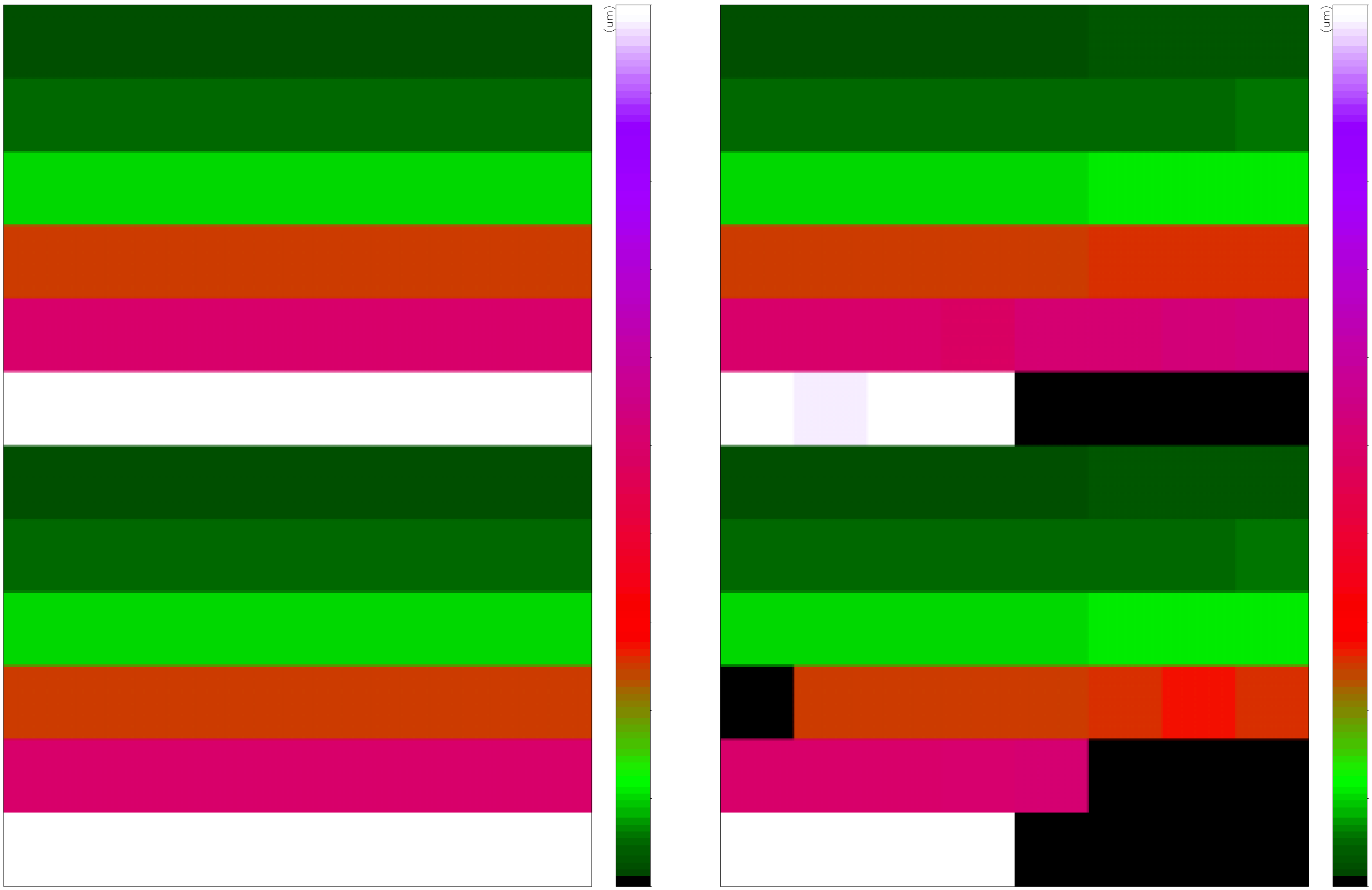

Figure 10: Snow Grain Size. LEFT PANEL: Input data. RIGHT PANEL: Retrieved results.

Validation – Synthetic Data (5)

Figure 11: Snow Impurity. LEFT PANEL: Input data. RIGHT PANEL: Retrieved results.

Validation – Synthetic Data (6)

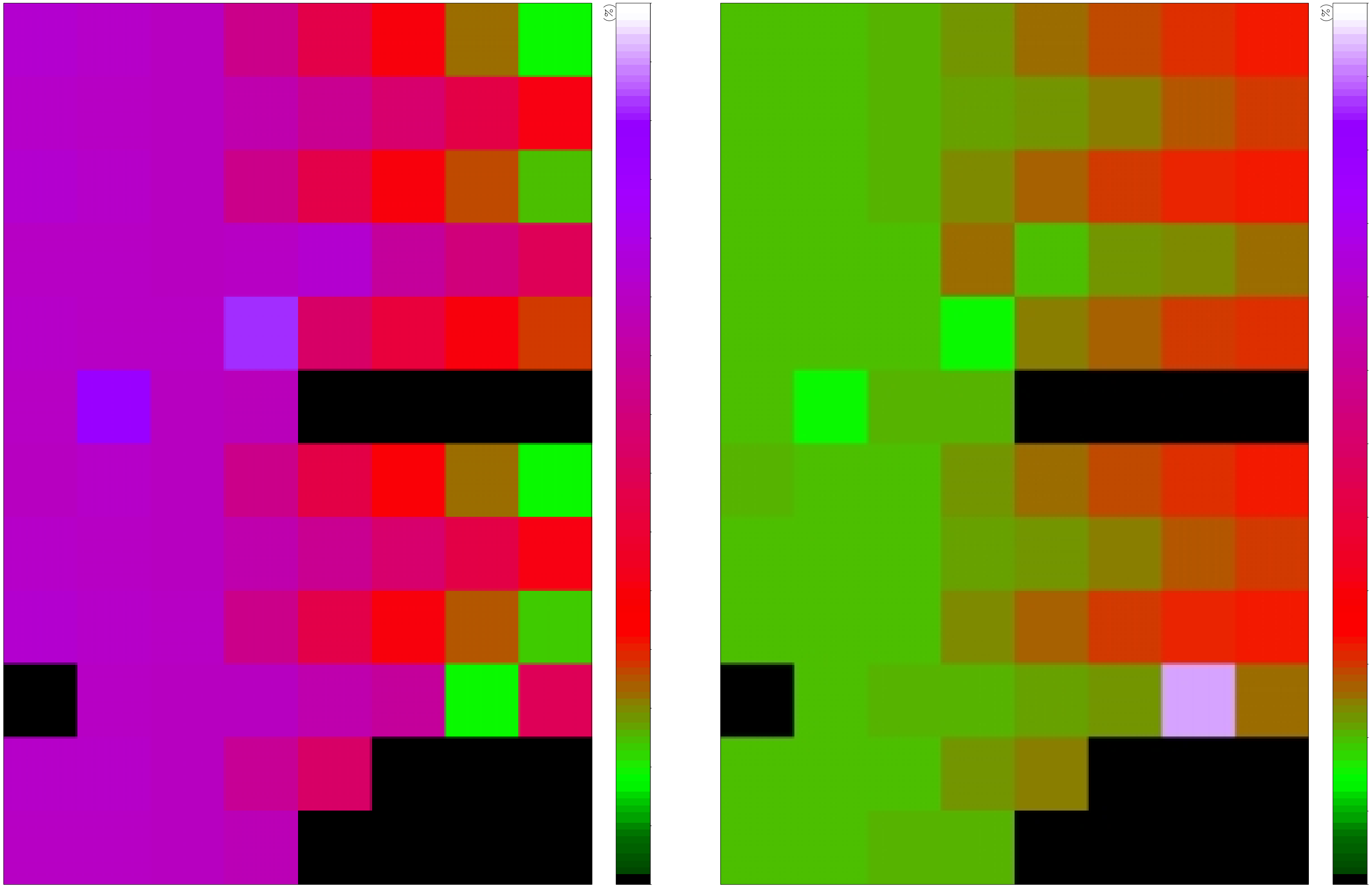

Figure 12: Retrieval (%). LEFT PANEL: Grain Size. RIGHT PANEL: Impurity.

MODIS Data –Greenland (1)

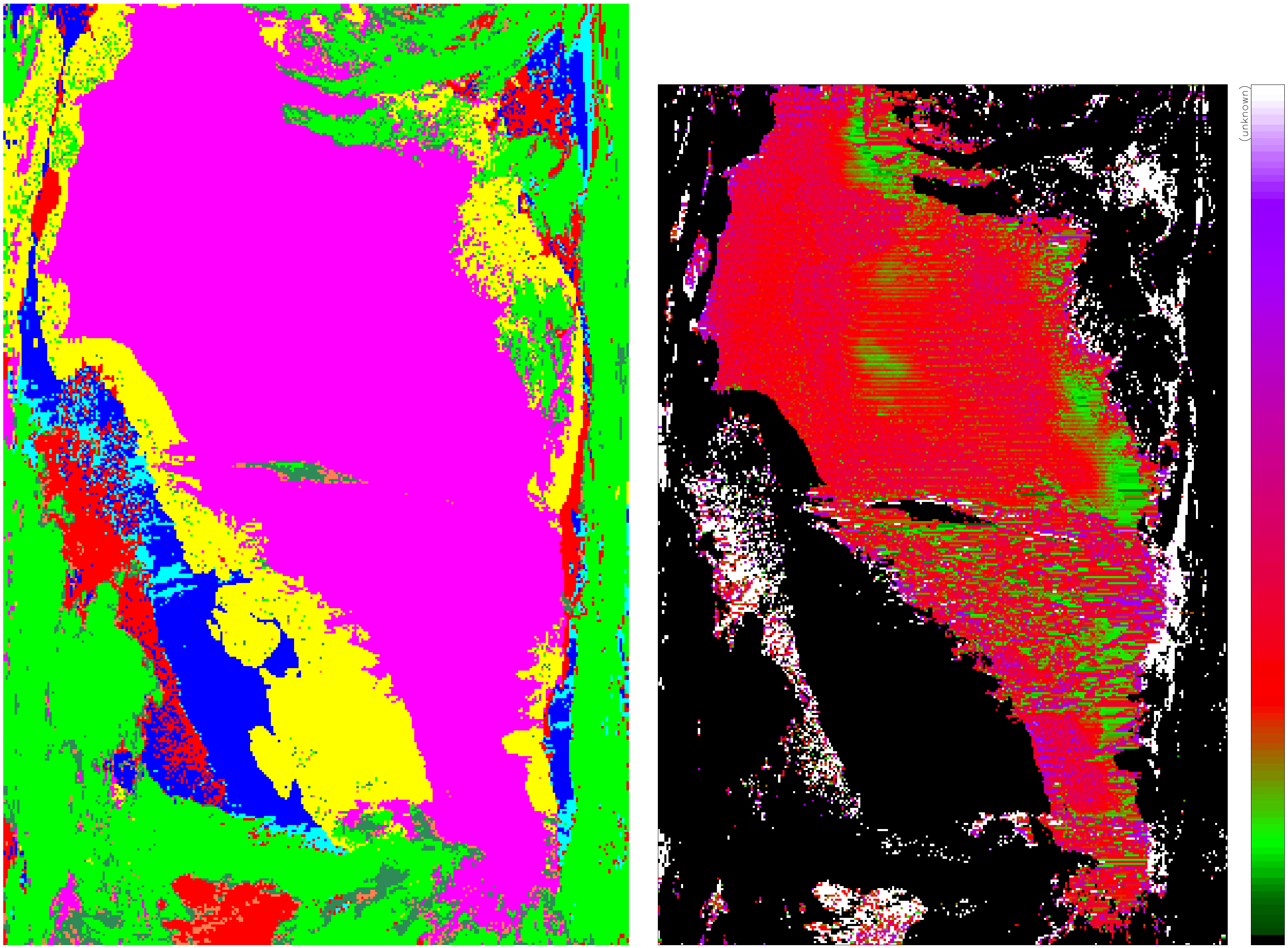

Figure 13: LEFT PANEL: Cloud mask. RIGHT PANEL: Aerosol optical depth. Retrieved from MODIS data on June 18, 2000 over Greenland..

MODIS Data –Greenland (2)

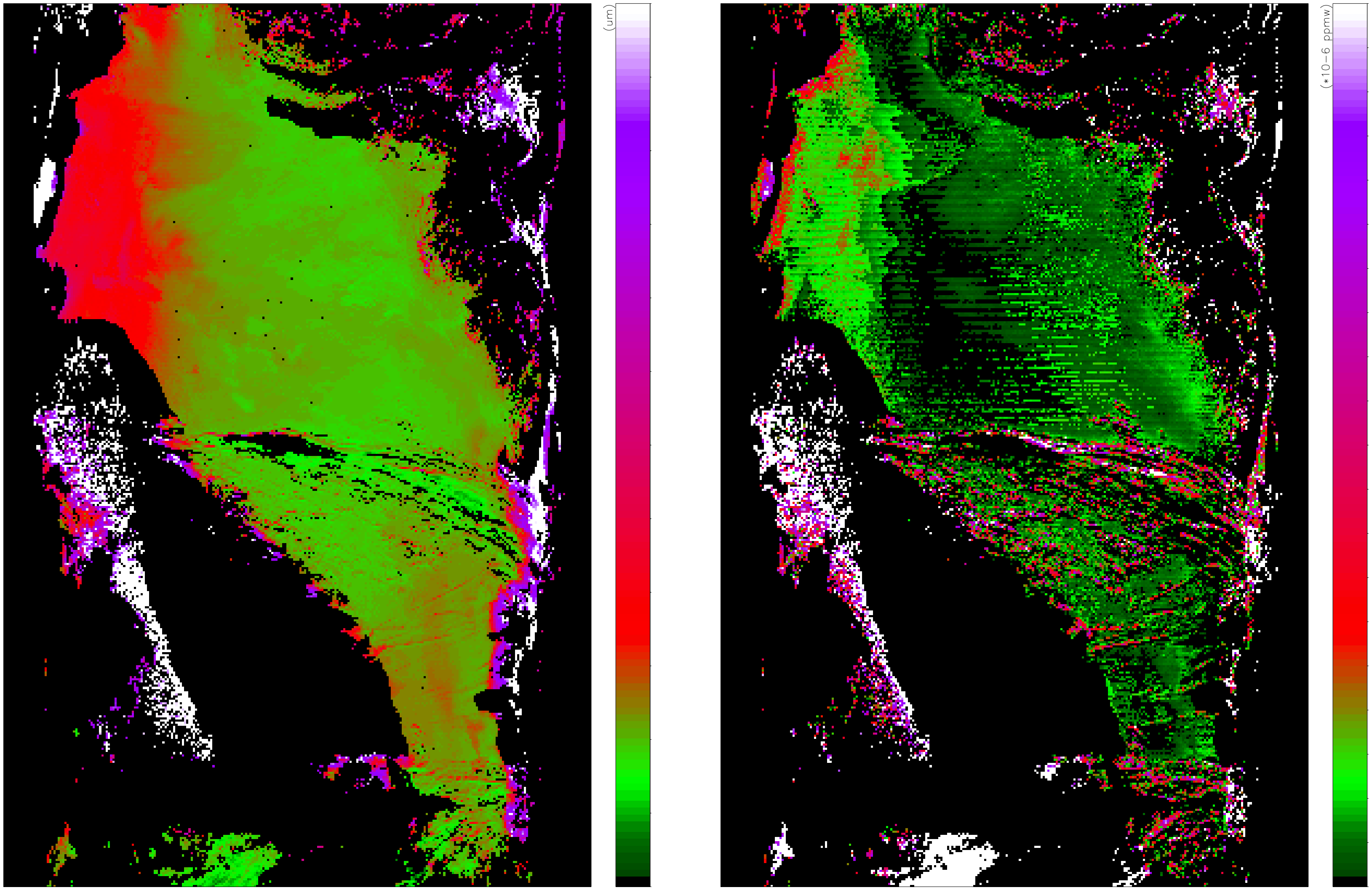

Figure 14: LEFT PANEL: Grain size. RIGHT PANEL: Snow impurity concentration. Retrieved from MODIS data on June 18, 2000 over Greenland.

MODIS Data – Central United States (1)

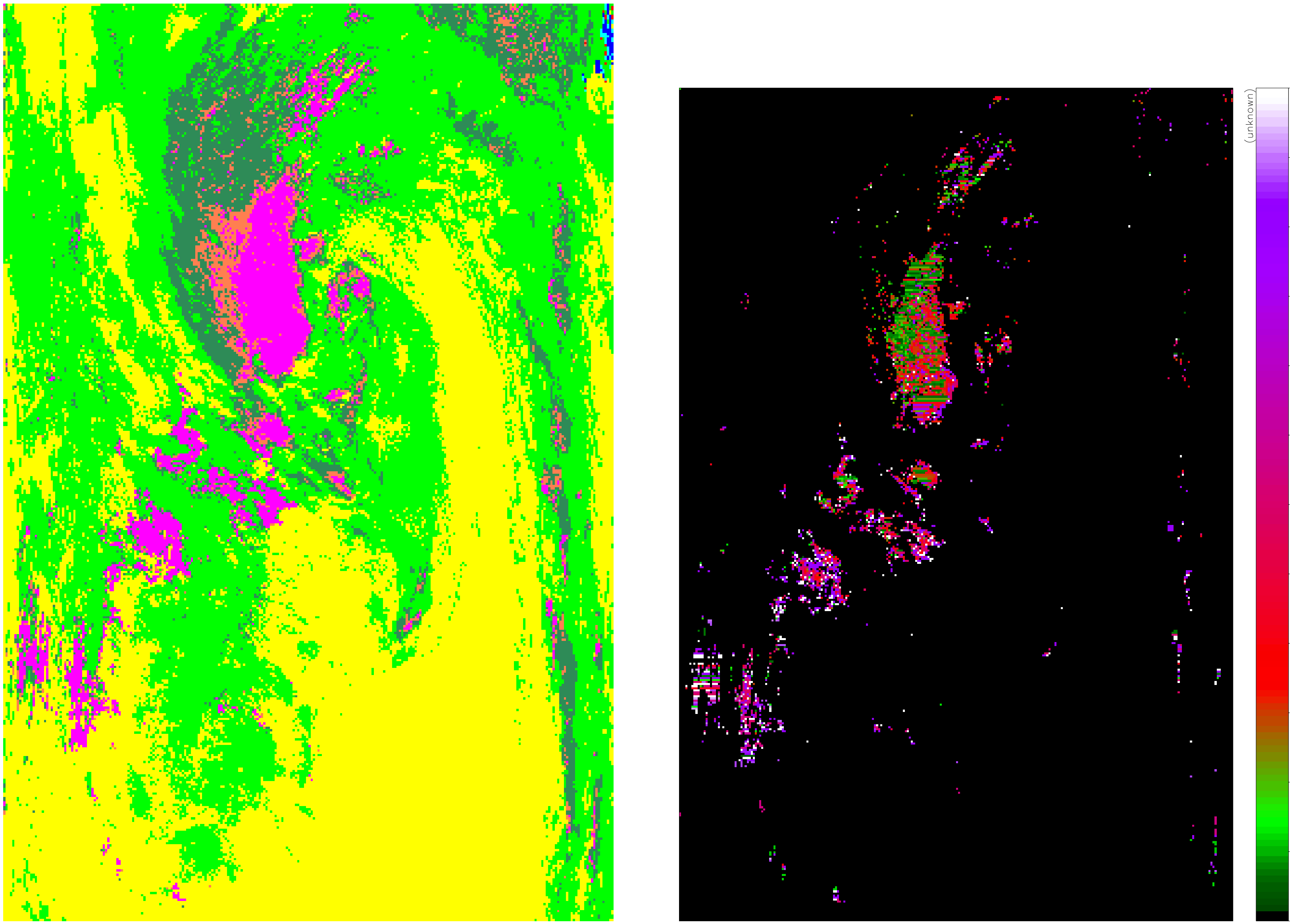

Figure 15: LEFT PANEL: Cloud mask. RIGHT PANEL: Aerosol optical depth. Retrieved from MODIS data on November 2, 2000 over United States.

MODIS Data – Central United States (2)

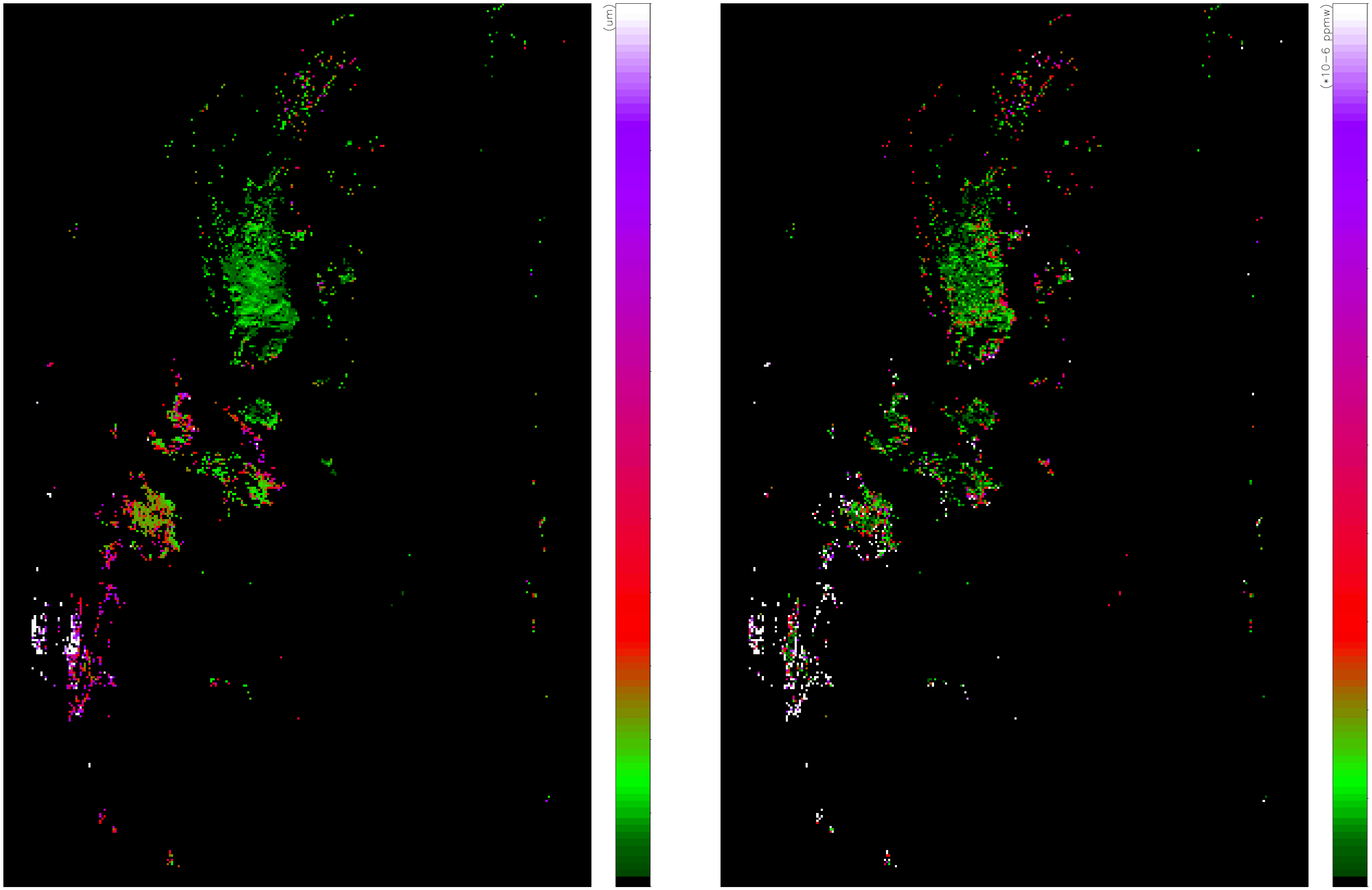

Figure 16: LEFT PANEL: Grain size. RIGHT PANEL: Snow impurity concentration. Retrieved from MODIS data on November 2, 2000 over United States.

Summary

In summary:

- **We have reviewed the snow grain size and retrieval algorithm with an emphasis on atmospheric correction issues.**
- **It has been tested against synthetic data and appears to be robust. Application to MODIS data yields reasonable results.**
- **Testing against field data is necessary when GLI data become available.**

These algorithms can be used to provide:

- **Cloud mask**
- **Aerosol optical properties**
- **Snow grain size and impurities**
- **Spectral albedo**

References

1. Li, W, K. Stamnes, B. Chen, and X. Xiong, Retrieval of the depth dependence of snow grain size from near-infrared radiances at multiple wavelengths, Geophys. Res. Lett., 28, 1699-1702, 2001.

2. Stamnes, K., S.C. Tsay, W. Wiscombe, and K. Jayaweera, 1988: Numerically stable algorithm for discrete-ordinate-method radiative transfer in multiple scattering and emitting layered media. *Appl. Opt.*, 27, 2502-2509.

3. Thomas, G. E. and K. Stamnes, 1999: *Radiative Transfer in the Atmosphere and Ocean* (Cambridge University Press).

4. Stamnes, K., S.C. Tsay, W. Wiscombe, and I. Laszlo, 2000: NASA report: DISORT, a General-Purpose Fortran Program for Discrete-Ordinate-Method Radiative Transfer in Scattering and Emitting Layered Media: Documentation of Methodology. The report as well as the Fortran code is available at: ftp://climate.gsfc.nasa.gov/pub/wiscombe/Multiple_Scatt/

5. Press, W.H., S.A. Teukolsky, W.T. Vetterling, and B.P. Flannery, 1986: *Numerical Recipes in Fortran 77* (Cambridge University Press).